




Article

# Remote Sensing of Coral Bleaching Using Temperature and Light: Progress towards an Operational Algorithm

William Skirving<sup>1,2,\*</sup>, Susana Enríquez<sup>3</sup> , John D. Hedley<sup>4,5</sup>, Sophie Dove<sup>6,7</sup>,  
C. Mark Eakin<sup>1</sup> , Robert A. B. Mason<sup>6,7</sup>, Jacqueline L. De La Cour<sup>1,8</sup> , Gang Liu<sup>1,8</sup>,  
Ove Hoegh-Guldberg<sup>7,9</sup>, Alan E. Strong<sup>1</sup>, Peter J. Mumby<sup>7,10</sup> and Roberto Iglesias-Prieto<sup>3,11</sup>

<sup>1</sup> Coral Reef Watch, National Oceanic and Atmospheric Administration, College Park, MD 20740, USA; Mark.Eakin@noaa.gov (C.M.E.); Jacqueline.Shapo@noaa.gov (J.L.D.L.C.); Gang.Liu@noaa.gov (G.L.); Alan.E.Strong@noaa.gov (A.E.S.)

<sup>2</sup> ReefSense Pty Ltd., Townsville, QLD 4814, Australia

<sup>3</sup> Unidad Académica de Sistemas Arrecifales Puerto Morelos, Instituto de Ciencias del Mar y Limnología, Universidad Nacional Autónoma de México, Cancun 77580, Mexico; susana.enriquezdominguez@gmail.com (S.E.); rzi3@psu.edu (R.I.-P.)

<sup>4</sup> Numerical Optics Ltd., Tiverton EX16 8AA, UK; j.d.hedley@gmail.com

<sup>5</sup> School of Biosciences, Exeter University, Exeter EX4 4PS, UK

<sup>6</sup> Coral Reef Ecosystems Laboratory, School of Biological Sciences, University of Queensland, St. Lucia, QLD 4072, Australia; sophie@uq.edu.au (S.D.); robert.mason1@uq.net.au (R.A.B.M.)

<sup>7</sup> ARC Centre of Excellence for Coral Reef Studies, University of Queensland, St. Lucia, QLD 4072, Australia; oveh@uq.edu.au (O.H.-G.); p.j.mumby@uq.edu.au (P.J.M.)

<sup>8</sup> Global Science & Technology, Inc., Greenbelt, MD 20740, USA

<sup>9</sup> Global Change Institute, University of Queensland, St. Lucia, QLD 4072, Australia

<sup>10</sup> Marine Spatial Ecology Lab, School of Biological Sciences, University of Queensland, St. Lucia, QLD 4072, Australia

<sup>11</sup> Department of Biology, The Pennsylvania State University, University Park, PA 16802, USA

\* Correspondence: William.skirving@noaa.gov; Tel.: +61-4-0489-3406

Received: 3 October 2017; Accepted: 19 December 2017; Published: 22 December 2017

**Abstract:** The National Oceanic and Atmospheric Administration's Coral Reef Watch program developed and operates several global satellite products to monitor bleaching-level heat stress. While these products have a proven ability to predict the onset of most mass coral bleaching events, they occasionally miss events; inaccurately predict the severity of some mass coral bleaching events; or report false alarms. These products are based solely on temperature and yet coral bleaching is known to result from both temperature and light stress. This study presents a novel methodology (still under development), which combines temperature and light into a single measure of stress to predict the onset and severity of mass coral bleaching. We describe here the biological basis of the Light Stress Damage (LSD) algorithm under development. Then by using empirical relationships derived in separate experiments conducted in mesocosm facilities in the Mexican Caribbean we parameterize the LSD algorithm and demonstrate that it is able to describe three past bleaching events from the Great Barrier Reef (GBR). For this limited example, the LSD algorithm was able to better predict differences in the severity of the three past GBR bleaching events, quantifying the contribution of light to reduce or exacerbate the impact of heat stress. The new Light Stress Damage algorithm we present here is potentially a significant step forward in the evolution of satellite-based bleaching products.

**Keywords:** coral bleaching; Light Stress Damage; LSD; DHW; remote sensing of coral bleaching; NOAA Coral Reef Watch; CRW; mass coral bleaching; light stress;  $F_v/F_m$

## 1. Introduction

Corals live in an endosymbiotic relationship with unicellular algae forming what is referred to as the “holobiont”. These dinoflagellate algae (genus *Symbiodinium*), collect light and perform photosynthesis, transferring energy to the coral. Coral bleaching refers to the dramatic loss of the *Symbiodinium* population that inhabits coral tissues, leaving the coral polyps transparent and making visible the underlying white calcium carbonate skeleton. This occurs when the symbiosis breaks down under any stressful condition that pushes the symbiosis beyond its limits of stability. The causes or “stressors” can include but are not restricted to: anomalous temperature (both hot and cold), anomalous increasing levels of light, anomalous levels of salinity (both high and low), reduction in water quality (e.g., heavy metals) and diseases [1–7]. Additionally, partial loss of coral pigmentation can occur during acclimation to high-light conditions [8–10] or too low nutrient availability [11]. Seasonal changes in the number of symbionts [12,13] and/or in symbiont pigmentation [14] can also lighten coral color during summer but these changes are unrelated to symbiosis instability. It is therefore important to distinguish between coral bleaching and coral holobiont homeostatic adjustments to the environment, since bleaching not only involves a dramatic change in coral pigmentation but is also an indication of a dysfunctional condition of the symbiotic relationship.

All the stressors listed above are known to cause bleaching on small to medium “local” scales (i.e., less than synoptic). However, heat stress is directly linked to synoptic-scale climate events and therefore is the only stressor demonstrated to have the capacity to cause mass coral bleaching (i.e., encompassing hundreds or more square kilometers and affecting many reefs at once). The first documented bleaching event was recorded in the 1870s [1] and the first recorded bleaching event attributed to heat stress was in 1911 [15]. Since the late 1970s the number, scale and intensity of coral bleaching events have grown significantly. While the first basin-scale (and possibly global) bleaching event occurred during the 1982–1983 El Niño [16,17], the first bleaching event demonstrated to have a fully global impact was not until 1998 [18]. Since the 1998 global coral bleaching event, heat stress events have occurred somewhere in the world each year and large-scale severe events are becoming more frequent, with subsequent global events in 2010 and 2014–2017 [19]. This trend has been linked to elevated ocean temperatures due to anthropogenic climate change [5,18].

To better understand the implications of climate change for coral communities, it is important to develop adequate tools to monitor these large-scale bleaching events and the stress that causes them. In doing so, we can compare the extent, duration and severity of different mass bleaching events in relation to physical disturbances and to the areas, coral communities and/or species particularly affected. This knowledge in combination with a better understanding of coral physiology and the cellular mechanisms that explain coral bleaching will help us to better model and predict the future risk to reefs from climate change, which will enable the development and encourage the adoption of better management tools and practices.

The National Oceanic and Atmospheric Administration’s (NOAA) Coral Reef Watch program (CRW) developed and operates the world’s only operational global satellite products designed specifically to monitor bleaching-level heat stress. Seawater temperature anomalies above the local maximum monthly mean (*MMM*); the average temperature of the climatologically-hottest month of the year [20] have been recognized to be the principal cause for mass coral bleaching events [5,21]. The HotSpot (*HS*) product, developed in 1997, is a sea surface temperature (*SST*) anomaly product comparing current *SST* to the *MMM*. In its current form, it provides a measure of the level of daily heat stress on corals [22,23]. This product was followed in 2000 with a near real-time satellite product called the Degree Heating Week (*DHW*), which provides a measure of the accumulated heat stress and has been shown to be an accurate predictor of coral bleaching [22–24].

These satellite-based coral bleaching products were designed to help coral reef managers identify and monitor oceanic heat stress and hence better predict mass coral bleaching. These products have been demonstrated to perform well when used to describe the onset of coral bleaching [25,26]. However, they occasionally predict bleaching for coral reefs where the phenomenon was not observed and vice

versa. The products are based solely on SST and yet mass coral bleaching is known to be a result of the combined effect of temperature and light on the photosynthetic activity of *Symbiodinium* [27–30]. Indeed, mass bleaching has failed to materialize under persistently cloudy conditions despite the existence of sustained elevated sea temperatures that would otherwise elicit coral bleaching [31].

This paper describes a methodology that is planned to underpin a major evolution of the NOAA CRW satellite products. This new methodology (called Light Stress Damage, or LSD) enables satellite-derived SST data to be combined together with satellite-derived solar insolation data in a scientifically valid way. The LSD algorithm is based on physiological processes that incorporate the synergistic effects of light and elevated temperature to induce coral bleaching. Such stress causes a significant decline in holobiont photosynthetic performance due to the accumulation of light-induced damage to the photosynthetic apparatus (photodamage) [28–30] and can be used to measure the photodamage of *Symbiodinium*, even prior to visible bleaching. The LSD methodology is novel in that it allows the quantification of the severity of a particular heat stress event as a function of the variation in the magnitude of photodamage accumulation derived from the amplification of light stress under elevated temperature. Light stress is defined as the condition where the energy absorbed by the photosynthetic apparatus of a coral-algal symbiont exceeds its photoprotective abilities, causing photodamage accumulation. This excess energy also causes *Symbiodinium* to activate mechanisms to acclimate to high light [32,33]. Since light stress depends on the photoacclimatory condition of *Symbiodinium*, this algorithm also includes the effect of coral photoacclimation to counterbalance the enhancement of light stress during a heat stress event.

It is hoped that the LSD product will provide a more accurate measure of the onset and severity of a coral heat-stress event, allowing for improved bleaching predictions with dramatically reduced false positives. Improved characterization of the timing and levels of stress are expected to improve the predictions (in near real-time as well as hindcast) of the severity and mortality associated with mass bleaching events of scleractinian corals.

The development of the LSD algorithm took advantage of work being done at Universidad Nacional Autónoma de México (UNAM) in Puerto Morelos. The experiments carried out at UNAM were performed independently of the work described in this paper. Preliminary results from these experiments have been used in an opportunistic manner to guide the method by which light and temperature have been combined to form the LSD algorithm. The main purpose of this paper is to provide a description of this methodology and its nuances. An example of the application of the LSD algorithm is provided mainly to clarify the methodology but it also serves to demonstrate that the LSD algorithm has potential to provide improved bleaching predictions when compared to methods that use temperature only.

#### *Coral Response to Variable Solar Irradiance*

The amount of light available for photosynthesis (photosynthetically available radiation or PAR) rapidly increases from near zero just before dawn to a maximum at the local solar noon (on clear days) and then drops off to be near zero again just after dusk. The amount of light available for coral photosynthesis varies with cloudiness, sea surface roughness, water turbidity, depth and local shading.

Photosynthetic rates of *Symbiodinium* increase linearly with light at low irradiance levels and then gradually diminish until saturation ( $E_k$ ) at a maximum rate ( $P_{max}$ ) [34]. The slope of this linear increase (photosynthetic efficiency,  $\alpha$ ),  $E_k$  and  $P_{max}$  vary among coral species and photoacclimatory conditions. The amount of energy absorbed by the photosynthetic apparatus above the saturation level ( $E_k$ ) cannot be incorporated into the photosynthetic processes and thus it has to be dissipated as heat by means of different photoprotective mechanisms.  $E_k$  is a key descriptor of the photoacclimatory condition of the photosynthetic apparatus, as it determines the amount of solar energy absorbed in excess by *Symbiodinium* and varies significantly among and within *Symbiodinium* species. Its variability is regulated by the plasticity of the species' photosynthetic response to light changes but it is also

dependent on many other environmental changes that potentially affect photosystem II (PSII) excitation pressure and consequently the photoacclimatory response of the organism [35].

Photoprotection of the photosynthetic apparatus of all photosynthetic organisms requires continuous activity of cellular mechanisms for the repair of photodamage [36]. When the rate of damage to PSII exceeds the rate of repair, the photosynthetic apparatus accumulates photodamage, which is reflected in an incomplete diurnal recovery of the maximum PSII photochemical efficiency, measured as  $F_v/F_m$ , where  $F_v/F_m$  is the ratio of the difference between maximum fluorescence and minimum fluorescence ( $F_v$ ) to the maximum fluorescence ( $F_m$ ) as measured by a pulse amplitude modulated (PAM) fluorometer. This reduction in  $F_v/F_m$  can be used as a descriptor of photodamage accumulation at the level of the photosynthetic membrane [37,38].  $F_v/F_m$  as employed here is a good descriptor of the balance between the rate of accumulation of heat- and light-damaged PSII and their rate of repair [39].

As PSII damage accumulates, it results in the leakage of reactive oxygen species into the coral host, with the consequent increase in coral tissue oxidative stress [40]. Once photodamage accumulation and/or photosynthesis inhibition crosses a physiological threshold for the stability of the holobiont, the symbiotic relationship can break down leading to coral bleaching. The breakdown can also occur when the algal symbiont no longer contributes nutritionally to the symbiosis, causing the coral to expel them from its tissues [41]. After the stressful conditions abate and if the coral host is able to cope with the physiological perturbation [42], *Symbiodinium* is able to re-populate the living coral tissue. However, if the conditions were sufficiently severe to cause irreversible cellular damage, polyps may not survive the heat stress event and eventually die. Stressed corals also are more susceptible to disease [43].

The highest value for  $F_v/F_m$  achieved by the photosynthetic apparatus of *Symbiodinium* is around 0.7 (70% efficiency) [10,39,44,45], substantially lower than the maximum value of 0.89 that can be achieved by higher plants [46]. Accumulated photodamage causes a drop in  $F_v/F_m$ . Once the accumulation of damaged PSII induces a dramatic reduction in *Symbiodinium* population (i.e., coral bleaching), the recovery rate of  $F_v/F_m$  will be dependent on PSII repair of the surviving algae and/or the repopulation of *Symbiodinium* [47,48].

Reduction in  $F_v/F_m$  is also associated with the high-light photoacclimatory response to reduce PSII pressure [49,50]. Whilst there are photoacclimatory mechanisms that involve photochemical quenching, only photoacclimation involving an upregulation of non-photochemical quenching, such as the accumulation of inactive PSII (a population of PSII that engage solely in mitigating excess excitation energy via heat dissipation), will reduce  $F_v/F_m$  [51]. The rate of inactive PSII accumulation and the consequent reduction in  $F_v/F_m$  is proportional to the light absorbed in excess by the photosynthetic membranes of the algae [52]. According to this physiological background, two main parameters need to be generated to quantify photodamage: the first describes the amount of excess solar energy absorbed by a symbiont that significantly contributes to increased rates of PSII photoinactivation, called Excess Excitation Energy ( $EEE$ , mol quanta  $m^{-2} day^{-1}$ ); and the second is the amount of photodamage accumulated (i.e., inactive PSII).  $EEE$  varies with (1) light availability; (2) the holobiont's saturation irradiance threshold ( $E_k$ ); and (3) holobiont capacity for photoprotection and repair. It then follows that  $EEE$  represents a convenient quantitative descriptor of the severity of light stress, including that induced by heat stress. This impact can be calculated as the diurnal change in  $F_v/F_m$ , which reflects the diurnal photodamage accumulation in *Symbiodinium*.

The premise that heat stress will enhance the impact of  $EEE$  and PSII photoinactivation in *Symbiodinium*, with the consequent negative effect on photosynthetic activity of the holobiont, is based on evidence that light stress and photosynthetic inhibition are key components of the adverse impact of heat stress on the physiology of symbiotic corals [28–30,44]. Photosynthesis is a temperature-dependent process, especially at the upper tolerance threshold, as photosynthesis can drop dramatically with rising temperature [53–55]. Such fast photosynthesis decline induces a quick  $EEE$  rise and subsequent PSII photodamage accumulation. Accordingly, heat stress will enhance the effect of  $EEE$  and PSII

photoinactivation in *Symbiodinium*, with the consequent negative effect on the photosynthetic activity of the coral holobiont. After the stress is removed, processes allow  $F_v/F_m$  to recover, with  $F_v/F_m$  in stressed corals returning to the maximum value of 0.7 each year during the cool season [56].

To model this biological process, we have developed the Light Stress Damage (LSD) algorithm that combines *PAR* and *SST* to predict the impact of heat stress events on symbiotic corals. This algorithm allows quantification of energy available in excess for *Symbiodinium* as it is not possible to directly measure the energy in excess absorbed by *Symbiodinium* from satellite data. We quantified its negative impact on the symbiotic population using relative changes in  $F_v/F_m$ , due to variations in *PAR* and *SST* [37,38]. The LSD algorithm was derived from a combination of physiological processes and several empirical relationships determined by experimental manipulation of Caribbean corals. Thus, it describes key physiological relationships between  $F_v/F_m$  changes and the variation of *EEE* under optimal conditions and different levels of *PAR* and heat stress. The synergistic effects of light and temperature on  $F_v/F_m$  changes were combined into one index of light-induced damage equivalents (i.e., LSD index), with the aim of improving on the *DHW* measure of stress as an indicator of coral bleaching. As discussed below, constraints were placed on the form of the LSD algorithm so that it can be implemented on satellite data.

## 2. Methods

### 2.1. Definition of Relative $F_v/F_m$

The variation of the maximum photochemical efficiency ( $F_v/F_m$ ) of each day was calculated as relative  $F_v/F_m$  (rel  $F_v/F_m$ ) between two consecutive days:

$$\text{rel } F_v/F_m = [F_v/F_m]_{\text{today}} / [F_v/F_m]_{\text{yesterday}} \quad (1)$$

All modeled  $F_v/F_m$  values are subsequently derived from these relative values.

### 2.2. Photoacclimation

Photoacclimation in *Symbiodinium* occurs continuously and needs to be accounted for in the LSD algorithm. Anthony and Hoegh-Guldberg [57] found that photoacclimation in *Turbinaria mesenterina* occurred over a period of 5–10 days and provided figures for the daily acclimation of  $P_{\text{max}}$ . These assumed that acclimation rate is proportional to the difference between the current  $P_{\text{max}}$ , ( $P_{\text{max}}(t)$ ) and the  $P_{\text{max}}$  that would be optimal for constant light at the current level ( $P_{\text{maxS}}$ ),

$$dP_{\text{max}}/dt = \varepsilon(P_{\text{maxS}} - P_{\text{max}}(t)) \quad (2)$$

where  $t$  is measured in days. Anthony and Hoegh-Guldberg [57] quoted four resulting values for  $\varepsilon$ , two for acclimation upward (to higher light levels) and two for downward, ranging from 0.101 to 0.164. The associated standard errors suggest taking a single value for the upward and downward photoacclimation as the mean of 0.13 is reasonable, this corresponds to 50% acclimation in 5 days. However, that study suggested that upward and downward acclimation rates are not necessarily the same. This is an important topic for future research as the LSD algorithm and subsequent satellite products are still under development.

### 2.3. Definition of *EEE*

Excess Excitation Energy (*EEE*) is directly linked to the particular acclimatory and adaptive characteristics of an individual coral. This makes it impossible to use space-borne sensors for direct measurements. However, for any species or acclimatory condition,  $EEE = 0$  implies that the organism is well acclimated to the environment and no net light-stress has occurred (no photodamage has been accumulated). On both a daily as well as a seasonal basis, *Symbiodinium* need to cope with a continuously changing light environment that combines days where they receive more sunlight than

they can actually use for photosynthesis with days that allow net recovery. Thus, a useful proxy for daily  $EEE$  is the difference between daily  $PAR$  and the level of  $PAR$  to which a coral is acclimated. Hence, for the purpose of this paper,  $EEE$  will be defined as being the difference between  $PAR$  today and the coral's acclimated  $PAR$  level.

#### 2.4. Definition of HotSpot

The HotSpot ( $HS$ ) product, developed in 1997 by NOAA CRW, is a sea surface temperature ( $SST$ ) anomaly product that measures the temperature ( $^{\circ}C$ ) above the local maximum monthly mean ( $MMM$ ); the average temperature of the climatologically-hottest month of the year [20].

#### 2.5. Experimental Quantification of the Synergistic Effect of Light and Temperature

To quantify the association between  $rel F_v/F_m$  and  $EEE$  and to incorporate the synergistic effect of temperature on the variation of  $EEE$ , we used results from a set of mesocosm experiments performed as part of another study at UNAM in Puerto Morelos for the species *Orbicella (Montastraea) annularis*. A description of the experimental design and methods can be found in [58]. The variation in  $F_v/F_m$  arising from these experiments is documented in [58] and the quantitative description of the combined effect of light and temperature used in the development of the LSD algorithm are the subject of a physiological paper, Enríquez (in prep.).

The results from these experiments provided this study with equations relating  $EEE$  to  $F_v/F_m$  for three separate temperatures (Figure 1) for coral colonies of *O. annularis*. These results will be described in detail by Enríquez (in prep.).

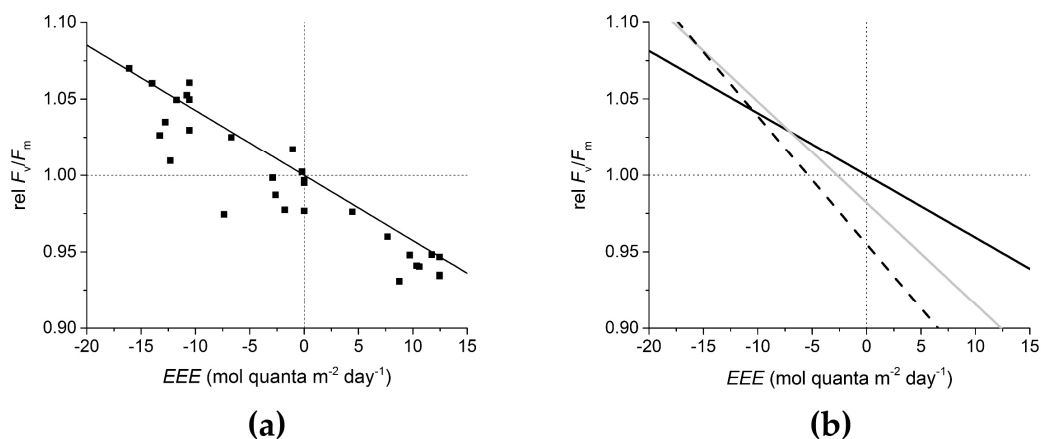


**Figure 1.** Experimental results for the variation of  $rel F_v/F_m$  as a function of the variation in  $EEE$  ( $\text{mol quanta m}^{-2} \text{ day}^{-1}$ ) for *Orbicella annularis* exposed to control conditions at (a)  $28^{\circ}C$  and (b) the results for three temperatures,  $28^{\circ}C$  (black),  $30^{\circ}C$  (grey) and  $32^{\circ}C$  (dashed). (Enríquez in prep.).

The results of these experiments are summarized in Figure 1. The plot of the data for the tank set at  $28^{\circ}C$  (Figure 1a) is representative of non-stressful temperatures for *O. annularis* in Puerto Morelos. It is therefore representative of corals whose variation in  $F_v/F_m$  is driven by  $EEE$  in the absence of heat stress. It describes the relationship for  $28^{\circ}C$  between  $rel F_v/F_m$  and  $EEE$  using the variation registered during 10 experimental days. Each data point is the average  $rel F_v/F_m$  (Equation (1)) on one evening over all corals for each light treatment.

For control conditions of no heat stress the relationship between  $rel F_v/F_m$  and  $EEE$  can be modeled by a linear regression (Figure 1a) giving:

$$rel F_v/F_m = 1.0 - 0.00426 EEE \quad (3)$$

The slope was derived from an unconstrained regression that produced a Y-intercept of 0.99, with  $R^2 = 0.86$  and standard error of the slope of 0.0003. However, the intercept in Equation (3) was set at 1.0 since, by definition,  $\text{rel } F_v/F_m = 1$  if  $EEE = 0$ .

As heat stress increases, the regression slopes become more negative and the Y-intercepts become progressively less than 1 (Figure 1b):

$$\begin{aligned} \text{i.e., at } 30^\circ\text{C } \text{rel } F_v/F_m &= 0.982 - 0.00663 \text{ } EEE \\ \text{at } 32^\circ\text{C } \text{rel } F_v/F_m &= 0.955 - 0.00837 \text{ } EEE \end{aligned}$$

Although research of the association between  $\text{rel } F_v/F_m$  and  $EEE$  under heat stress is still in progress, in order to test the idea behind the LSD algorithm, we have used these preliminary results from Enríquez (in prep.) to model the change in coefficients of this relationship as a function of the experimental HotSpots ( $HS$ ).

Using in situ data for the period 1992 to 2015 from the Puerto Morelos lagoon, the maximum of the monthly averages is  $29.8^\circ\text{C}$ . The  $MMM$  methodology requires this value to be re-centered on 1988.3 [59], which lowers the value to  $29.2^\circ\text{C}$ . Since the experiments were conducted with integer temperatures [58], the  $MMM$  used to derive  $HS$  should also be expressed as an integer. Hence, for the purpose of this paper, the  $MMM$  for Puerto Morelos is  $29^\circ\text{C}$  and since the control was set at  $28^\circ\text{C}$ , the resultant relationship between  $EEE$  and  $\text{rel } F_v/F_m$  (Equation (3)) is stable up until the  $MMM$  of  $29^\circ\text{C}$ . The two experimental levels of thermal stress were set at  $30^\circ\text{C}$  and  $32^\circ\text{C}$ , which are equivalent to HotSpots of 1 and 3 respectively. A linear regression was applied to each of the coefficients of the three experimental regression outputs, allowing the Y-intercepts and slopes (from Figure 1b) to be expressed in terms of HotSpots. The slopes of each of these regressions were used along with the known Y-intercepts (from Equation (3)), giving:

$$\text{Y-intercept} = 1 - 0.01164 \text{ } HS \quad (4)$$

$$\text{Slope} = -0.00426 - 0.00130 \text{ } HS \quad (5)$$

## 2.6. LSD Algorithm Description

The idea behind the LSD algorithm was to track the effects of  $EEE$  on photosystem efficiency throughout a bleaching season, taking into account the amplifying effects of anomalous temperature (i.e.,  $HS > 0$ ). A stress threshold is established using a multi-year time series of  $F_v/F_m$  due to the effects of  $EEE$  with no temperature effects (using Equation (3); explained in more detail below). After temperature effects were included with  $EEE$ , the  $F_v/F_m$  values occasionally dropped below this threshold. When that occurred, the corals experienced abnormally low  $F_v/F_m$  values, most likely due to heat-induced stress. To gain a measure of the total stress for an event, for all  $F_v/F_m$  values less than the threshold, the area between the  $F_v/F_m$  curve and the threshold was integrated and the total is called the LSD index.

## 3. Results

### 3.1. LSD Algorithm Demonstration

This demonstration of the application of the LSD algorithm is designed to better describe the algorithm rather than providing a definitive proof of the applicability of the algorithm to the generic prediction of coral bleaching. It also serves to explain the differences between the temperature-only DHW product and the light/temperature LSD product and why the inclusion of light is potentially an important evolution in satellite monitoring of environmental stress for prediction of coral bleaching.

Demonstrating the LSD algorithm required a location that had a long, continuous dataset of quality  $PAR$  measurements, reliable  $SST$  data and a complete and thorough set of in-water surveys to ensure that all bleaching and non-bleaching events were known. No such sites were found in the Caribbean; however, a useful site was located in the southern Great Barrier Reef at the Keppel Islands,

Australia (Figure 2). The near-by Rockhampton airport has a climate-quality light station operated by the Australian Bureau of Meteorology (BoM) from which the *PAR* data were sourced. *SST*s were available from the NOAA Advanced Very High Resolution Radiometer (AVHRR) satellite sensors [60] and tested against in situ data from the Australian Institute of Marine Science (AIMS) and since there was no difference in the below example for either data set, we chose to use the satellite *SST*. Lastly, AIMS have annual (or more frequent) surveys of the Keppel Islands corals. These islands also have a marine park ranger who reports any signs of coral stress. For the purpose of this demonstration, the period 1999 to 2006 was used.

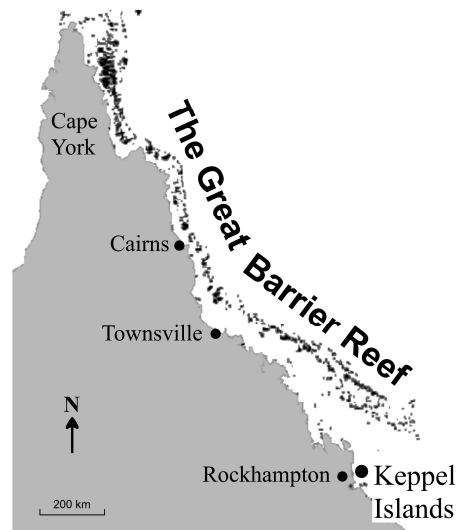


**Figure 2.** Map of Queensland showing the location of the Keppel Islands in the southern Great Barrier Reef and the township of Rockhampton.

The following presents an example of the application of the LSD algorithm. This example helps to demonstrate how the inclusion of light into the calculation of heat stress of corals can improve the determination of bleaching. Global implementation of the LSD algorithm will require testing its applicability in many more locations but since there is a scarcity of coral reef locations with sufficiently long time series of reasonable quality *PAR* measurements and *SST* measurements that are coincident with reliable bleaching reports, the validation of the general applicability of the LSD algorithm will be best done after implementation on satellite data (work currently in progress at NOAA CRW).

### 3.2. Definitions

A summary of all symbols and annotations used in the LSD algorithm example (below) can be found in Table 1.

**Table 1.** Summary of all symbols and annotations used in the LSD algorithm example.

Symbol	Description	Units
$i$	Day number	day
$PAR_i$	Daily integrated Photosynthetically Available Radiation on day $i$	$\text{mol quanta m}^{-2} \text{ day}^{-1}$
acclim $PAR_i$	$PAR$ to which the corals are currently acclimated on day $i$	$\text{mol quanta m}^{-2} \text{ day}^{-1}$
$EEE_i$	Daily Excess Excitation Energy on day $i$	$\text{mol quanta m}^{-2} \text{ day}^{-1}$
$F_v/F_m$	diurnal maximum PSII photochemical efficiency	-
rel $F_v/F_m$	change in $F_v/F_m$ relative to yesterday's $F_v/F_m = (F_v/F_m)_i / (F_v/F_m)_{i-1}$	-
$SST$	Sea Surface Temperature	$^{\circ}\text{C}$
$MMM$	Maximum Monthly Mean $SST$	$^{\circ}\text{C}$
$HS$	HotSpot = $SST - MMM$	$^{\circ}\text{C}$



### 3.3. Keppel Islands Example

To apply the LSD algorithm, first a seasonal  $F_v/F_m$  is calculated using *EEE* derived with *PAR* only (i.e., no temperature effect). This provides the LSD bleaching threshold. Next, the effects of temperature and light are included in the derivation of  $F_v/F_m$  by using a combination of *HS* and *PAR*. The results of this are then compared to the LSD bleaching threshold to derive the LSD index.

#### 3.3.1. Step 1: Derive the Daily Value of rel $F_v/F_m$ Due to *EEE* with No Temperature Effect

Daily total *PAR* was extracted from the Rockhampton BoM light station (Figure 3a). For this example, the LSD algorithm was set to 20 cm depth and an attenuation coefficient of  $K_d = 0.202 \text{ m}^{-1}$ , the average reported attenuation for *PAR* at inshore reefs of the Whitsunday Islands, just north of the Keppel Islands [61]. Like light, temperature varies through the water column, it therefore makes sense to set the light values to be vertically at the same level in the water column as the temperature values in order to avoid mismatches between *EEE* and *SST* effects that vary with water depth. Since the satellite *SST* data used by CRW are derived from measurements made at the sea surface and calibrated against drifting buoys [62], which provide temperatures at 20 cm depth [63], it follows that the light should also be set to a water depth of 20 cm.

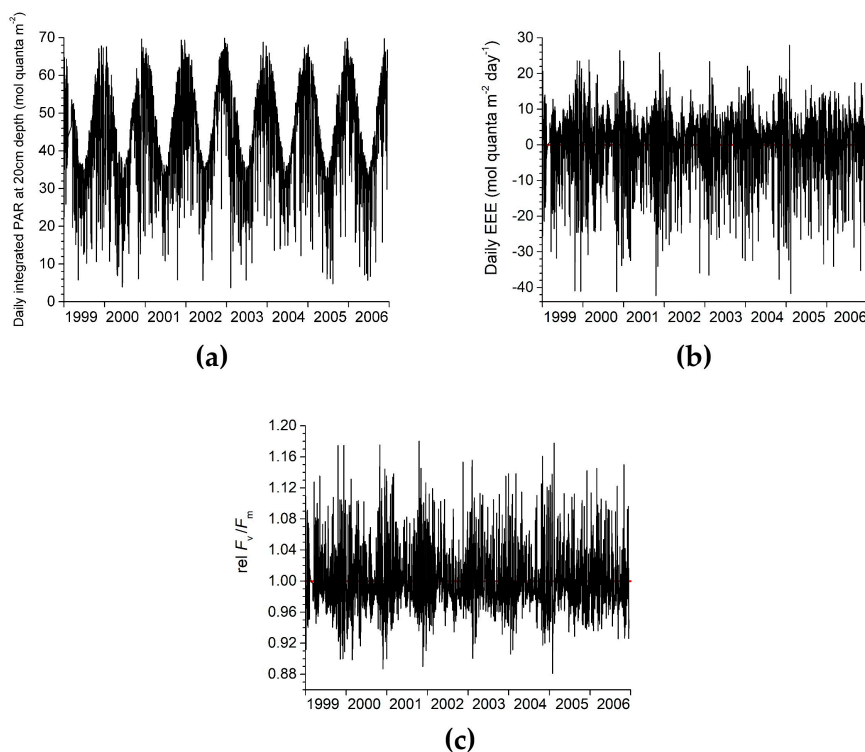


**Figure 3.** Rockhampton *PAR* at 20 cm depth (a), *EEE* (b) and change in relative  $F_v/F_m$  due to *EEE* with no heat stress (c) for the period 1999 to 2006.

The effect of light attenuation due to refraction and reflection at the sea surface was modeled prior to incorporation into the calculations. To cover both effects, NASA's Coupled Ocean and Atmosphere Radiative Transfer (COART, <http://cloudsgate2.larc.nasa.gov/jin/coart.html>) was used to simulate total daily *PAR* at the sea surface and at 1 cm below the surface. Since bleaching events often occur during low to no wind conditions [20] a wind speed of  $2 \text{ ms}^{-1}$  was chosen and a model resolution of  $0.01 \text{ } \mu\text{m}$  was used. The atmosphere in the model was set to "tropical" and the total downward flux of the combined direct and diffuse *PAR* was calculated at the surface and at a depth of 1 cm for each solar zenith angle from  $0^\circ$  to  $85^\circ$  at intervals of  $5^\circ$ . These were then totaled to simulate the total *PAR* for a day. The ratio of the daily total *PAR* at the surface vs the daily total at a depth of 1cm can then be

used to estimate the attenuation at the air/sea interface to be 0.964 (i.e., slightly less radiation reaches a depth of 1cm than is incident at the sea surface. This is mostly due to reflection).

At each daily step, the LSD algorithm simulated light acclimation (acclim  $PAR$ ) by determining the difference between the accumulated acclimation to  $PAR_{i-1}$  (i.e., acclim  $PAR_{i-1}$ ) and the actual  $PAR_i$ , the difference was then reduced by a factor of 0.13 to simulate the rate of daily acclimation [57]. Acclim  $PAR_i$  was then used to calculate  $EEE$ .

Acclimated  $PAR$  at 20 cm depth (Figure 3a) was calculated to obtain the daily value of rel  $F_v/F_m$  due to  $EEE$  with no temperature effect (Figure 3b):

$$EEE_i = PAR_i - \text{acclim } PAR_{i-1} \quad (6)$$

$$\text{where acclim } PAR_i = \text{acclim } PAR_{i-1} + 0.13(PAR_i - \text{acclim } PAR_{i-1}) \quad (7)$$

These values were then converted to rel  $F_v/F_m$  using Equation (3) (Figure 3c).

### 3.3.2. Step 2: Derive the Daily Variation in $F_v/F_m$ Due to $EEE$ (with No Temperature Effect)

The daily rel  $F_v/F_m$  variation was used to calculate daily values of  $F_v/F_m$  throughout the year using Equation (8):

$$(F_v/F_m)_i = (F_v/F_m)_{i-1} (\text{rel } F_v/F_m)_i \quad (8)$$

However, when Equation (8) was applied with no constraints, the resultant  $F_v/F_m$  values converged towards zero (Figure 4a). This is due to the asymmetry of  $EEE$  (Figure 3b). The bias towards negative anomalies resulted in the maximum for each consecutive year being progressively less than the previous year. To overcome this, at each winter solstice we assume that damage to the photosystems due to light stress was at a minimum and we reset  $F_v/F_m$  to 0.7, as being representative of the highest efficiency for *Symbiodinium*. This ensures that the seasonality described in [56] was reproduced in the model output.

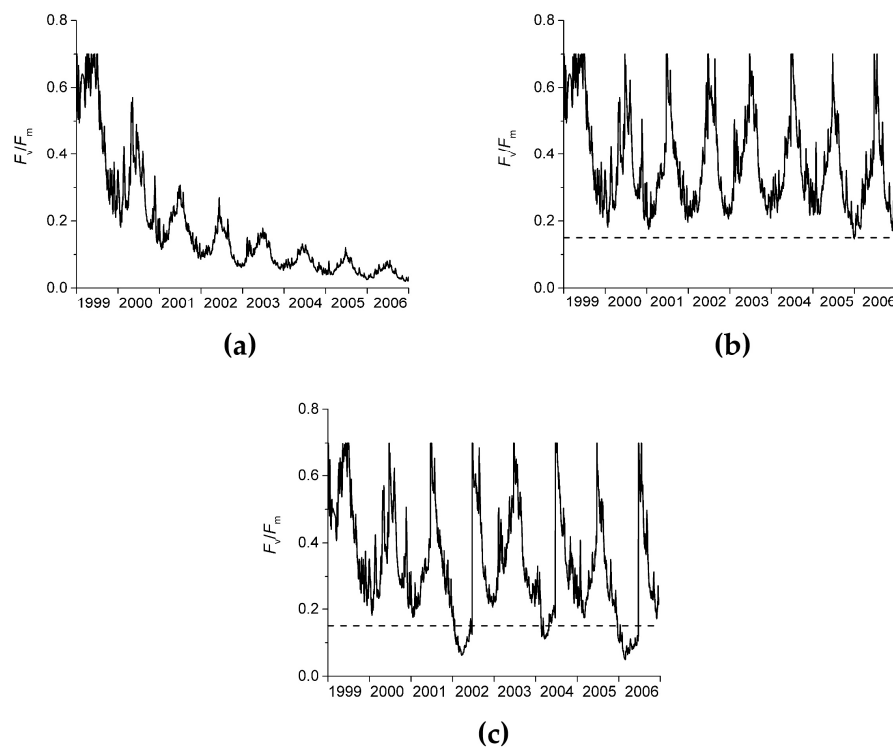


**Figure 4.** Seasonal variation of  $F_v/F_m$  over the period 1999 to 2006 with no annual reset and no heat stress (a), with annual reset and no heat stress (b) and with annual reset and heat stress (c). NB: the dashed line in (b,c) is the bleaching threshold of 0.15.

In keeping with the winter solstice reset, we also applied an upper limit to prevent  $F_v/F_m$  values from exceeding 0.7.

The reset value of 0.7 is somewhat arbitrary and may not be representative for *Symbiodinium* in all regions, however due to the makeup of the LSD algorithm presented here, changing this value does not alter the success of the algorithm, only its interpretation (i.e., the output graphs all look the same if another value is used but the range of the Y-axis alters). When applying the LSD algorithm to global satellite data it is likely necessary to use 0.7 in all regions so as to maintain a consistent interpretation of outputs from each region.

Starting with an  $F_v/F_m$  value of 0.7 at the winter solstice, Equation (9) was used to calculate values plotted in Figure 4b:

$$(F_v/F_m)_i = \text{minimum}((F_v/F_m)_{i-1} (\text{rel } F_v/F_m)_i, 0.7) \quad (9)$$

The long-term minimum of  $F_v/F_m$  over the 8-year dataset was then used as the bleaching threshold, since it was expected that the corals have adapted to the local non-stressful (“normal”) light conditions. Hence, light on its own should be able to drive the photosystem to the threshold of stress but not beyond.

This established the bleaching threshold for shallow corals in the Keppel Islands as 0.15 (Figure 4b).

Figure 4b demonstrates that the LSD algorithm reproduced the seasonality in  $F_v/F_m$  reported by [56] and that it is reproducing realistic values that vary according to field observations of  $F_v/F_m$ .

### 3.3.3. Step 3: Derive the Daily Value of $\text{rel } F_v/F_m$ Due to *EEE*, Including Temperature Effects

Night-time SST values were derived from the NOAA AVHRR and plotted for the period of 1999 to 2006 in Figure 5a. HotSpot values were then calculated using *MMM*, where  $MMM = 27.5^\circ\text{C}$ , after the NOAA CRW methodology [20,63] and are plotted in Figure 5b.

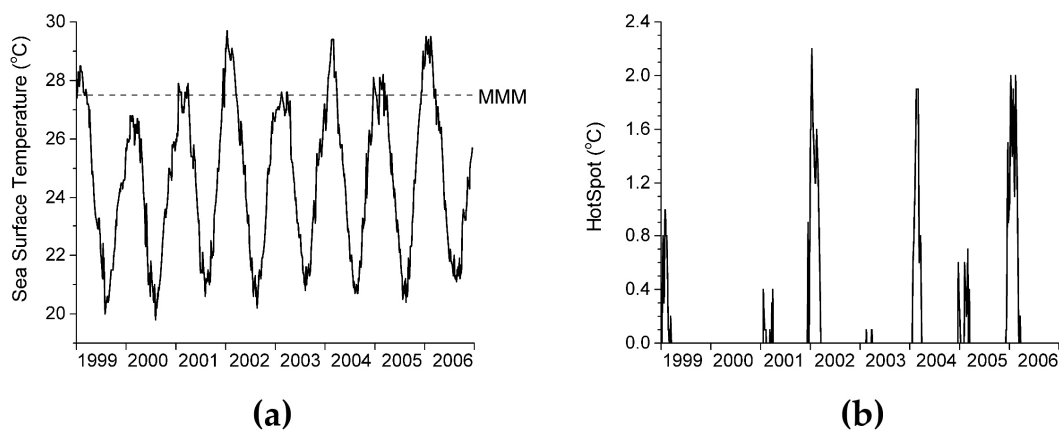


**Figure 5.** Plot of SST (a) and HotSpot anomaly (b) for the period 1999 to 2006.

For each day Equations (4) and (5) were used to calculate  $\text{rel } F_v/F_m$  for *EEE* including the effects of temperature.

$$\text{i.e., } (\text{rel } F_v/F_m)_i = (1 - 0.01164 HS_i) + (-0.00426 - 0.00130 HS_i) EEE_i$$

### 3.3.4. Step 4: Derive the Daily Variation in the Absolute Values of $F_v/F_m$ Due to *EEE*, Including Temperature Effects

Daily  $F_v/F_m$  was then calculated using Equation (9), only this time,  $\text{rel } F_v/F_m$  includes the effects of temperature via step 3. As in Step 1, at each winter solstice,  $F_v/F_m$  was reset to the upper limit for

$F_v/F_m$  of 0.7. The results are plotted in Figure 4c. Note that when adding the effect of temperature,  $F_v/F_m$  values occasionally drop below the stress threshold of 0.15, indicating bleaching-level stress.

### 3.3.5. Step 5: Calculate the Light Stress Damage Index

The LSD index is summed from the day on which  $F_v/F_m$  drops below the light stress threshold (0.15, determined in step 2, above) and continued to be summed until  $F_v/F_m$  rises above the stress threshold. The LSD index is therefore, a measure of the total accumulated stress during each stress event, derived by integrating between the  $F_v/F_m$  curve and the stress threshold (for all  $F_v/F_m < threshold$ ). This is similar to the methodology CRW uses for the calculation of *DHW* from *HS*.

The LSD index for this example is the integration between the 0.15 threshold and those  $F_v/F_m$  values less than 0.15:

$$LSD = \sum x_i, \text{ where } x_i = threshold - (F_v/F_m)_i; x_i \geq 0 \quad (10)$$

From Figure 4c it can be seen that there were three occasions when the  $F_v/F_m$  dropped below 0.15, in 2002, 2004 and 2006. However, the LSD index accumulation for 2004 is very small (Figure 6a).

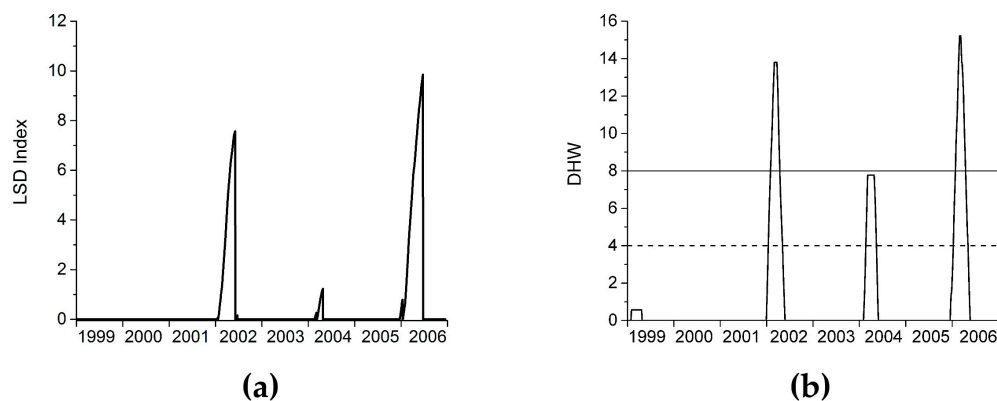


**Figure 6.** Plot of Accumulated Light Stress Damage (a) and Degree Heating Weeks (b) for the Keppel Islands between 1999 and 2006. NB: 2002 and 2006 were bleaching years; the corals paled in 2004 with no bleaching; and all other years were stress-free. The dashed line in plot (b) at  $DHW = 4$ , is the threshold above which ecologically significant bleaching is expected. The solid horizontal line at  $DHW = 8$ , represents the threshold for widespread severe bleaching with some mortality.

For comparison purposes, *DHW* values were calculated using *HS* for the Keppel Islands for the period 1999 to 2006, using the methodology described in [20], see Figure 6b. Note that the *DHW* index is more pronounced than the LSD index for 2004.

## 4. Discussion

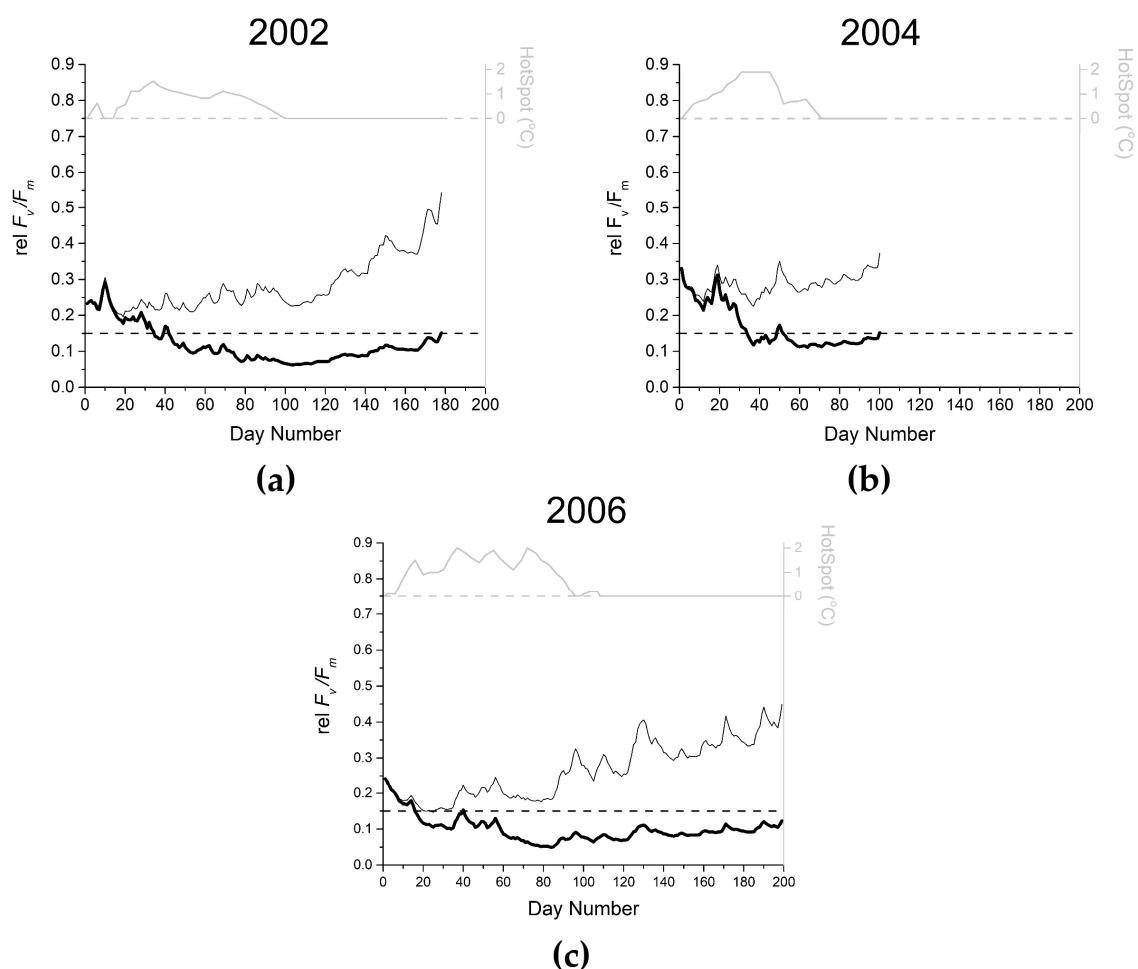
The LSD index (Figure 6a) suggest that there were two major stress events on the Keppel Islands during the period of 1999 to 2006. This was confirmed by annual surveys conducted by the Australian Institute of Marine Science (AIMS), in which only two bleaching events were recorded, one in early 2002 (100% bleached, 26% mortality) and the other in early 2006 (100% bleached, 35% mortality) (Australian Institute of Marine Science, unpublished data). The only other year in this record that came close to a bleaching event was in early 2004 when corals were recorded as having paled but not bleached and showed no mortality. The LSD index (Figure 6a) shows 2004 as a relatively small accumulation of light stress.

Figure 6b is a plot of the corresponding *DHW* values for the Keppel Islands over 1999 to 2006. Using the accepted key thresholds for the interpretation of the *DHW* product (*DHW* of 4 indicates ecologically significant bleaching and a *DHW* value of 8 or more indicates severe bleaching) [20,25]. These interpretations suggest that Figure 6b is indicating that the bleaching events in 2002 and 2006

were severe and of similar magnitude and that there was an ecologically significant bleaching event in 2004, which bordered on being classified as a severe bleaching event.

The 2004 heat event provides a good example where the use of temperature alone can lead to a false positive. A significant temperature anomaly existed in terms of the daily HotSpot (Figure 5b) and in terms of accumulated temperature anomalies in the DHW product (Figure 6b). However, surveys observed paling with no bleaching or mortality.

The LSD index more accurately predicted the 2002 and 2006 bleaching events (indicating that 2002 was significantly less severe than 2006) and a small amount of stress in 2004. Figure 7 shows three plots, one for each of the three temperature anomaly events experienced at the Keppel Islands in 2002, 2004 and 2006. The top grey line in each of the three plots shows the HS values, allowing visual identification of when temperature influenced the  $F_v/F_m$  values. The lower two black graphs in each of the plots are of  $F_v/F_m$ , with no heat stress effect (EEE-only, thin black line) and with the addition of the effect of heat stress (thick black line).



**Figure 7.** Plots of the three stress events in 2002 (a), 2004 (b) and 2006 (c). Plots are all on the same scale for easy comparison. Within each plot, the top (grey) line graph is the daily HotSpot values with the scale on the right of each plot. The two black line plots are  $F_v/F_m$  for the effect of EEE-only (thin black line) and for the combined effect of light and heat (thick black line).

The three plots in Figure 7 clearly demonstrate the influence that light has on the accumulation of heat stress (for the Keppel Island example) and why the outcomes for 2002, 2004 and 2006 were so different between the LSD index and DHW products. In general, the story is one of light buffering. When light conditions leading into the heat stress event are favorable (i.e., when EEE is consistently

small), it is possible for these conditions to provide a “buffer” against the effects of the heat stress, allowing the corals to cope with larger amounts of heat stress before feeling its effects.

Figure 6b shows that the heat stress, as measured by DHW, was similar for 2002 (DHW = 13.8) and 2006 (DHW = 15.2). However, Figure 7a shows the *EEE*-only stress starting at around 0.25 and steadily rising over the period of the heat anomaly, serving to provide a modest buffer and hence, reducing the heat stress accumulation, resulting in an LSD value of 7.6. During 2006 however, Figure 7c shows the *EEE*-only stress starting at around 0.24 (similar to the 2004 level), however unlike 2004 where the *EEE*-only stress improved throughout the heat stress event, in 2006 it dipped right down to the stress threshold, providing no buffer for coral stress, allowing the full impact of heat stress to be felt by the corals. This resulted in an LSD value of 9.9, which is 30% larger than the 2004 value. The 2006 DHW value is only 10% larger than the 2004 value.

Since the AIMS data report both events having had 100% bleaching, the only measure of severity we can use is the level of mortality. 2006 had 35% mortality which is 35% larger than the mortality in 2004 of 26%. At least for this example, the LSD index seemed to do a marginally better job of characterizing these two bleaching events than did DHW.

It is the 2004 heat stress event that demonstrates the potential of the LSD algorithm. Figure 6b indicates that the DHW product recorded 7.8 in 2004, which was sufficient to have caused ecologically significant bleaching (above DHW of 4) and was bordering on being classed as a severe bleaching event (above DHW of 8) [20,25]. This is out of step with the AIMS bleaching records, which indicate that the corals paled with no bleaching. The LSD index recorded 1.2, which is only 15% of the 2002 LSD index. Had the 2004 DHW value been 15% of its 2002 value then it would have recorded a DHW value of 2, which equates to stress with no significant bleaching.

Figure 7b explains why the DHW product overstated the level of stress in 2004 while the LSD index provided a good measure of the level of stress.

In 2004, at the start of the heat event,  $F_v/F_m$  due to *EEE*-only was around 0.3 and although it fluctuated,  $F_v/F_m$  due to *EEE*-only remained quite high throughout the event. This countered the effect of the temperature anomaly and prevented  $F_v/F_m$  from dropping to the bleaching threshold until well into the heat stress event. As a result, the LSD only accumulated a small amount of stress. With light levels playing such a major role in offsetting the heat stress for this event, it is not surprising that the *DHW* product did not accurately describe this event.

These three stress events clearly demonstrate the important role of light in the lead up to and during a heat stress event. Favorable light conditions (i.e., consistently low *EEE* values to maintain a relatively high  $F_v/F_m$  value) in the lead up to a heat event can provide a significant buffer against temperature anomalies, allowing corals to be less susceptible to the effects of elevated temperatures, as they were during the 2004 Keppel Islands example. However, the converse can also occur as in the 2006 example, where only slightly higher temperature anomalies generated quite different outcomes in the severity and length of the stress event due to the lack of a light buffer because of unfavorable light conditions leading up to the event (i.e., consistently high *EEE* values, which pushed the  $F_v/F_m$  values close to the stress threshold at the beginning of the heat event).

The LSD was therefore able to take into account the impact of light on corals and their *Symbiodinium* and determine how much stress (i.e., combined effects of light and temperature) is needed during the temperature anomaly event to induce coral bleaching, significantly improving the ability to predict total stress when compared to a purely temperature derived stress index, such as the *DHW* product. Differences in the combined light and heat stress measured in the LSD index predicted both the bleaching and mortality much better than heat stress measured in the *DHW*.

As promising as the LSD algorithm is, there is still work to be done before the algorithm is complete. For instance, if the daily  $F_v/F_m$  value, within the LSD algorithm, is not reset to 0.7 at the winter solstice,  $F_v/F_m$  values converged towards zero after several years. This occurred in the calculation using *EEE* with no temperature effect, as well as when temperature was combined with *EEE*. While the annual reset worked for the production of a predictive algorithm, it was based on

empirical observations rather than physiological mechanisms. Sensitivity testing identified two places where the addition of new terms to the LSD algorithm could prevent the need for this reset. The first was in the use of 0.13 as the daily acclimation rate [57]. This study suggested that acclimation rates may not be the same for increasing and decreasing light levels. We tested the application of asymmetric values and reducing the response to decreasing light by 5–10% stabilized the  $F_v/F_m$  over the eight-year period. This demonstrated that the multi-year stability of  $F_v/F_m$  was very sensitive to slight changes in the symmetry of the photoacclimation rate. However, imposing such a change did not stabilize the multi-year  $F_v/F_m$  simulation after a heat stress event. This suggested a term is needed to simulate the recovery of *Symbiodinium* after heat stress has ended. Both the physiological recovery of the photosynthetic apparatus through the up-regulation of the repair mechanisms and the recovery of *Symbiodinium* populations through asexual reproduction can contribute to this recovery. This can be simulated by maintaining the enhanced rate of recovery found in the slope of heat-stressed corals (Figure 1) for a period after heat stress has ended. It is reasonable to expect that this period of enhanced recovery may be maintained for up to 30 days [47,48]. Imposing such a change stabilized the multi-year  $F_v/F_m$  simulation after a heat stress event and was relatively insensitive to the length of time over which enhanced recovery was applied. It may be possible to quantify and include these two terms once the LSD algorithm is applied to remotely-sensed data (currently underway at NOAA) and a larger dataset becomes available for their derivation.

NOAA has a global PAR product that matches the temporal and spatial resolution of its 0.05 degree (approx. 5 km) Geo-Polar Blended SST product. Information about the GOES Surface and Insolation Products (GSIP) can be found at [www.ospo.noaa.gov/Products/land/gsip/index\\_v3.html](http://www.ospo.noaa.gov/Products/land/gsip/index_v3.html). Currently, there is 11 years of satellite-derived PAR data for the eastern Pacific and the Caribbean/Gulf of Mexico regions. Global coverage has been available since March 2014, however when the switch from MTSAT to Himawari-8 (Japanese geostationary satellites over the Australasian region) occurred on 5 December 2015, the GSIP product was not updated to account for Himawari-8 data. The inclusion of Himawari-8 data within the GSIP product is planned and will take place in the near future.

NOAA CRW have also been working closely with many collaborators (in particular the University of British Columbia) to collate a global dataset of quality controlled in-water coral bleaching observations against which to calibrate and validate algorithms such as the LSD and DHW.

When the PAR and SST satellite data sets are combined with the quality-controlled in-water bleaching observations, the path for continued development of the LSD algorithm will be in good shape.

## 5. Conclusions

The new methodology described herein will be used to underpin a new satellite product within the NOAA CRW coral bleaching decision support system.

The Keppel Islands example demonstrates that this methodology shows great promise to improve upon the already successful DHW heat stress product. However, more work is needed before the LSD index will be ready for use as an operational satellite product, including testing its applicability across multiple coral species and habitats around the world.

Changes in light attenuation with depth and through time (due to episodic events such as floods) will influence  $F_v/F_m$  and how it interacts with temperature variability. This can have important impacts on the LSD algorithm. These interactions will need to be investigated in the near future and are a planned step in the development of the LSD as a remotely-sensed product.

Time of acclimation to light for positive vs negative  $EEE$  is also important for the LSD algorithm and will need to be resolved before this algorithm can reach its full potential.

The Keppel Islands example helped to explain the LSD algorithm and why it works, rather than to provide a definitive test of the algorithm's ability to predict coral bleaching. Testing its applicability on other locations and species is fundamental to test the predictive capacity of the LSD algorithm for coral bleaching. However, considering the scarcity of quality in situ light data near coral reefs

with documented bleaching records, this validation will have to wait until the algorithm has been fully implemented on satellite data, work currently underway at NOAA. Such work will need to consider both the light reaching the ocean surface and the reduction in light as it passes through seawater to reach the coral. For many applications, full implementation of the LSD algorithm for remote sensing may require not only temperature and surface insolation data but also the application of ocean color products that measure changes in light attenuation in the water column—products also in development at NOAA.

**Acknowledgments:** Development of NOAA Coral Reef Watch’s Light Stress Damage product suite was supported by the NOAA Coral Reef Conservation Program (CRCP), the Australian Research Council, the University of Queensland and the Universidad Nacional Autónoma de México. The scientific results and conclusions, as well as any views or opinions expressed herein, are those of the author(s) and do not necessarily reflect the views of NOAA or the Department of Commerce.

**Author Contributions:** William Skirving, Susana Enríquez, Roberto Iglesias-Prieto, Sophie Dove and John Hedley were the main contributors to the concepts in this paper, with C. Mark Eakin, Robert A. B. Mason, Ove Hoegh-Guldberg, Alan E. Strong and Peter J. Mumby making smaller but significant contributions to the concepts in this paper. All experiments included in this paper were conducted by Susana Enríquez and involved Roberto Iglesias-Prieto, results from other experiments conducted by Robert A. B. Mason and involving Sophie Dove were not used in this work but did influence the concepts and algorithm development. Most of the algorithm development was performed by William Skirving, Susana Enríquez and Roberto Iglesias-Prieto, with significant input from John Hedley, C. Mark Eakin, Robert A. B. Mason and Sophie Dove. The manuscript was mostly written by William Skirving, Susana Enríquez and Roberto Iglesias-Prieto, with significant contributions being made by John Hedley, C. Mark Eakin, Sophie Dove, Robert A. B. Mason, Jacqueline L. De La Cour and Gang Liu.

**Conflicts of Interest:** The authors declare no conflict of interest. The founding sponsors had no role in the design of the study; in the collection, analyses, or interpretation of data; in the writing of the manuscript and in the decision to publish the results.

## References

1. Glynn, P.W. Coral Reef Bleaching: Facts, Hypothesis and Implications. *Glob. Chang. Biol.* **1996**, *2*, 495–509.
2. Lesser, M.P. Elevated temperature and ultraviolet radiation cause oxidative stress and inhibit photosynthesis in symbiotic dinoflagellates. *Limnol. Oceanogr.* **1996**, *41*, 271–283. [[CrossRef](#)]
3. Brown, B.E. The significance of pollution in eliciting the ‘bleaching’ response in symbiotic cnidarians. *Int. J. Environ. Pollut.* **2000**, *13*, 392–415. [[CrossRef](#)]
4. Douglas, A.E. Coral Bleaching—How and why? *Mar. Pollut. Bull.* **2003**, *46*, 385–392. [[PubMed](#)]
5. Hoegh-Guldberg, O. Climate change, coral bleaching and the future of the World’s coral reefs. *Mar. Freshw. Res.* **1999**, *50*, 839–866.
6. Hoegh-Guldberg, O.; Fine, M.; Skirving, W.; Johnstone, R.; Dove, S.; Strong, A. Coral bleaching following wintry weather. *Limnol. Oceanogr.* **2005**, *50*, 265–271. [[CrossRef](#)]
7. Dove, S.G.; Hoegh-Guldberg, O. The cell physiology of coral bleaching. In *Coral Reefs and Climate Change: Science and Management*; Phinney, J.T., Hoegh-Guldberg, O., Kleypas, J., Skirving, W., Strong, A., Eds.; American Geophysical Union: Washington, DC, USA, 2006; pp. 55–71.
8. Falkowski, P.G.; Jokiel, P.L.; Kinzie, R.A. Irradiance and Corals. In *Coral Reefs*; Dubinsky, Z., Ed.; Elsevier: Amsterdam, The Netherlands, 1990; pp. 89–107.
9. Iglesias-Prieto, R.; Trench, R.K. Acclimation and adaptation to irradiance in symbiotic dinoflagellates. I. Responses of the photosynthetic unit to changes in photon flux density. *Mar. Ecol. Prog. Ser.* **1994**, *113*, 163–175.
10. Hennige, S.J.; Suggett, D.J.; Warner, M.E.; McDougall, K.E.; Smith, D.J. Photobiology of *Symbiodinium* revisited: Bio-Physical and bio-optical signatures. *Coral Reefs* **2009**, *28*, 179–195.
11. Dubinsky, Z.; Stambler, N.; Ben-Zion, M.; McCloskey, L.; Muscatine, L.; Falkowski, P. The effect of external nutrient resources on the optical properties and photosynthetic efficiency of *Stylphora pistillata*. *Proc. R. Soc. Lond.* **1990**, *239*, 231–246.
12. Fagoonee, I.I.; Wilson, H.B.; Hassell, M.P.; Turner, J.R. The dynamics of zooxanthellae populations: A long-term study in the field. *Science* **1999**, *283*, 5403–843.



13. Fitt, W.K.; McFarland, M.E.; Warner, M.E.; Chilcoat, G.C. Seasonal patterns of tissue biomass and densities of symbiotic dinoflagellates and relation to coral bleaching. *Limnol. Oceanogr.* **2000**, *45*, 677–685. [[CrossRef](#)]
14. Brown, B.E.; Dunne, R.P.; Ambarsari, I.; Le Tissier, M.D.A.; Satapoomin, U. Seasonal fluctuations in environmental factors and variations in symbiotic algae and chlorophyll pigments in four Indo-Pacific coral species. *Mar. Ecol. Prog. Ser.* **1999**, *191*, 53–69. [[CrossRef](#)]
15. Berkelmans, R.; De'ath, G.; Kinimonth, S.; Skirving, W. Coral bleaching on the Great Barrier Reef: Correlation with sea surface temperature, a handle on 'patchiness' and comparison of the 1998 and 2002 events. *Coral Reefs* **2004**, *23*, 74–83. [[CrossRef](#)]
16. Glynn, P.W. Widespread coral mortality and the 1982–83 El Niño warming event. *Environ. Conserv.* **1984**, *11*, 133–146. [[CrossRef](#)]
17. Coffroth, M.A.; Lasker, H.R.; Oliver, J.E. Coral mortality outside of the eastern Pacific during 1982–1983: Relationship to El Niño. In *Global Ecological Consequences of the 1982–83 El Niño-Southern Oscillation*; Glynn, P.W., Ed.; Elsevier Oceanography Series; Elsevier: Amsterdam, The Netherlands, 1989; pp. 141–182.
18. Wilkinson, C. (Ed.) *Status of Coral Reefs of the World*; Australian Institute of Marine Science: Townsville, Queensland, Australia, 2004.
19. Eakin, M.C.; Liu, G.; Gomez, A.M.; De La Cour, J.L.; Heron, S.F.; Skirving, W.J.; Geiger, E.F.; Marsh, B.L.; Tirak, K.V.; Strong, A.E. Ding, Dong, The Witch is Dead (?)—Three Years of Global Coral Bleaching 2014–2017. *Reef Encount.* **2017**, *32*, 33–38.
20. Skirving, W.J.; Strong, A.E.; Liu, G.; Liu, C.; Arzayus, F.; Sapper, J.; Bayler, E. Extreme events and perturbations of coastal ecosystems: Sea surface temperature change and coral bleaching. In *Remote Sensing of Aquatic Coastal Ecosystem Processes*; Richardson, L.L., LeDrew, E.F., Eds.; Springer: Dordrecht, The Netherlands, 2006; pp. 11–25.
21. Brown, B.E. Coral bleaching: Causes and consequences. *Coral Reefs* **1997**, *16*, 129–138. [[CrossRef](#)]
22. Liu, G.; Heron, S.F.; Eakin, C.M.; Muller-Karger, F.E.; Vega-Rodriguez, M.; Guild, L.S.; De La Cour, J.L.; Geiger, E.F.; Skirving, W.J.; Burgess, T.F.R.; et al. Reef-scale Thermal Stress Monitoring of Coral Ecosystems: New 5-km Global Products from NOAA Coral Reef Watch. *Remote Sens.* **2014**, *6*, 11579–11606. [[CrossRef](#)]
23. Liu, G.; Skirving, W.J.; Geiger, E.F.; De La Cour, J.L.; Marsh, B.L.; Heron, S.F.; Tirak, K.V.; Strong, A.E.; Eakin, C.M. NOAA Coral Reef Watch's 5 km Satellite Coral Bleaching Heat Stress Monitoring Product Suite Version 3 and Four-Month Outlook Version 4. *Reef Encount.* **2017**, *32*, 39–45.
24. Eakin, C.M.; Morgan, J.A.; Heron, S.F.; Smith, T.B.; Liu, G.; Alvarez-Filip, L.; Baca, B.; Bartels, E.; Bastidas, C.; Bouchon, C.; et al. Caribbean Corals in Crisis: Record Thermal Stress, Bleaching and Mortality in 2005. *PLoS ONE* **2010**, *5*, e13969. [[CrossRef](#)] [[PubMed](#)]
25. Heron, S.F.; Johnston, L.; Liu, G.; Geiger, E.F.; Maynard, J.A.; De La Cour, J.L.; Johnson, S.; Okano, R.; Benavente, D.; Burgess, T.F.R.; et al. Validation of Reef-scale Thermal Stress Satellite Products for Coral Bleaching Monitoring. *Remote Sens.* **2016**, *8*, 59. [[CrossRef](#)]
26. Kayanne, H. Validation of degree heating weeks as a coral bleaching index in the northwestern Pacific. *Coral Reefs* **2017**, *36*, 63. [[CrossRef](#)]
27. Iglesias-Prieto, R.; Matta, J.L.; Robins, W.A.; Trench, R.K. Photosynthetic response to elevated temperature in the symbiotic dinoflagellate *Symbiodinium microadriaticum* in culture. *Proc. Natl. Acad. Sci. USA* **1992**, *89*, 10302–10305. [[CrossRef](#)] [[PubMed](#)]
28. Jones, R.J.; Hoegh-Guldberg, O.; Larkum, A.W.D.; Schreiber, U. Temperature-induced bleaching of corals begins with impairment of the CO<sub>2</sub> fixation mechanism in zooxanthellae. *Plant Cell Environ.* **1998**, *21*, 1219–1230. [[CrossRef](#)]
29. Warner, M.E.; Fitt, W.K.; Schmidt, G.W. Damage to photosystem II in symbiotic dinoflagellates: A determinant of coral bleaching. *Proc. Natl. Acad. Sci. USA* **1999**, *96*, 8007–8012. [[CrossRef](#)] [[PubMed](#)]
30. Takahashi, S.; Nakamura, T.; Sakamizu, M.; van Woesik, R.; Yamasaki, H. Repair machinery of symbiotic photosynthesis as the primary target of heat stress for reef-building corals. *Plant Cell Phys.* **2004**, *45*, 251–255. [[CrossRef](#)]
31. Mumby, P.J.; Chisholm, J.R.M.; Edwards, A.J.; Andrefouet, S.; Jaubert, J. Cloudy weather may have saved Society Island reef corals during the 1998 ENSO event. *Mar. Ecol. Prog. Ser.* **2001**, *222*, 209–216. [[CrossRef](#)]
32. Niyogi, K. Photoprotection revisited: Genetic and molecular approaches. *Annu. Rev. Plant Physiol. Plant Mol. Biol.* **1999**, *50*, 333–359. [[CrossRef](#)] [[PubMed](#)]
33. Niyogi, K. Safety valves for photosynthesis. *Curr. Opin. Plant Biol.* **2000**, *6*, 455–460. [[CrossRef](#)]

34. Anderson, J.M.; Chow, W.S.; Park, Y.I. The grand design of photosynthesis: Acclimation of the photosynthetic apparatus to environmental cues. *Photosynth. Res.* **1995**, *46*, 129–139. [[CrossRef](#)] [[PubMed](#)]
35. Chalker, B. Simulating light-saturation curves for photosynthesis and calcification by reef-building corals. *Mar. Biol.* **1981**, *63*, 135–141. [[CrossRef](#)]
36. Melis, A. Photosystem II damage and repair cycle in chloroplasts: What modulates the rate of photodamage “in vivo”? *Trends Plant Sci.* **1999**, *94*, 130–135. [[CrossRef](#)]
37. Vass, I.; Styring, S.; Hundal, T.; Koivuniemi, A.; Aro, E.; Andersson, B. Reversible and irreversible intermediates during photoinhibition of photosystem II: Stable reduced  $Q_A$  species promote chlorophyll triplet formation. *Proc. Natl. Acad. Sci. USA* **1992**, *90*, 1408–1412. [[CrossRef](#)]
38. Vásquez-Elizondo, R.M.; Enríquez, S. Coralline algal physiology is more adversely affected by elevated temperature than reduced pH. *Sci. Rep.* **2016**, *6*, 19030. [[CrossRef](#)] [[PubMed](#)]
39. Hill, R.; Brown, C.M.; DeZeeuw, K.; Campbell, D.A.; Ralph, P.J. Increased rate of D1 repair in coral symbionts during bleaching is insufficient to counter accelerated photo-inactivation. *Limnol. Oceanogr.* **2011**, *56*, 139–146. [[CrossRef](#)]
40. Weis, V.M. Cellular mechanisms of Cnidarian bleaching: Stress causes the collapse of symbiosis. *J. Exp. Biol.* **2008**, *211*, 3059–3066. [[CrossRef](#)] [[PubMed](#)]
41. Titlyanov, E.A.; Titlyanova, T.V.; Leletkin, V.A.; Tsukahara, J.; van Woesik, R.; Yamazato, K. Degradation of zooxanthellae and regulation of their density in hermatypic corals. *MEPS* **2006**, *139*, 167–178. [[CrossRef](#)]
42. Dunn, S.R.; Pernice, M.; Green, K.; Hoegh-Guldberg, O.; Dove, S.G. Thermal Stress Promotes Host Mitochondrial Degradation in Symbiotic Cnidarians: Are the Batteries of the Reef Going to Run Out? *PLoS ONE* **2012**. [[CrossRef](#)] [[PubMed](#)]
43. Burge, C.A.; Eakin, C.M.; Friedman, C.S.; Froelich, B.; Hershberger, P.K.; Hofmann, E.E.; Petes, L.E.; Prager, K.C.; Weil, E.; Willis, B.L.; et al. Climate Change Influences on Marine Infectious Diseases: Implications for Management and Society. *Ann. Rev. Mar. Sci.* **2014**, *6*, 249–277. [[CrossRef](#)] [[PubMed](#)]
44. Iglesias-Prieto, R. Temperature-dependent inactivation of photosystem II in symbiotic dinoflagellates. In Proceedings of the 8th International Coral Reef Symposium, Panama City, Panama, 24–29 June 1996; Macintyre, I.G., Ed.; Smithsonian Tropical Research Institute: Balboa, Panama, 1997; pp. 1313–1318.
45. Warner, M.E.; LaJeunesse, T.C.; Robinson, J.D.; Thur, R.M. The ecological distribution and comparative photobiology of symbiotic dinoflagellates from reef corals in Belize: Potential implications for coral bleaching. *Limnol. Oceanogr.* **2006**, *51*, 1887–1897. [[CrossRef](#)]
46. Schreiber, U.; Bilger, W.; Neubauer, C. Chlorophyll fluorescence as a noninvasive indicator for rapid assessment of in vivo photosynthesis. In *Ecophysiology of Photosynthesis*; Schulze, E.D., Caldwell, M.M., Eds.; Springer: Berlin, Germany, 1995; pp. 49–70.
47. Rodríguez-Román, A.; Hernández-Pech, X.; Thomé, P.E.; Enríquez, S.; Iglesias-Prieto, R. Photosynthesis and light utilization in the Caribbean coral *Montastraea faveolata* recovering from a bleaching event. *Limnol. Oceanogr.* **2016**, *51*, 2702–2710. [[CrossRef](#)]
48. DeSalvo, M.K.; Sunagawa, S.; Fisher, P.; Voolstra, C.R.; Iglesias-Prieto, R.; Medina, M. Coral host transcriptomic states are correlated with *Symbiodinium* genotypes. *Mol. Ecol.* **2010**, *19*, 1174–1186. [[CrossRef](#)] [[PubMed](#)]
49. Maxwell, D.P.; Falk, S.; Huner, N.P.A. Photosystem II excitation pressure and development of resistance to photoinhibition. I. Light-harvesting complex II abundance and zeaxanthin content in *Chlorella vulgaris*. *Plant Phys.* **1995**, *107*, 687–694. [[CrossRef](#)]
50. Iglesias-Prieto, R.; Beltrán, V.H.; LaJeunesse, T.C.; Reyes-Bonilla, H.; Thomé, P.E. Different algal symbionts explain the vertical distribution of dominant reef corals in the eastern Pacific. *Proc. R. Soc. Lond.* **2004**, *271*, 1757–1763. [[CrossRef](#)] [[PubMed](#)]
51. Warner, M.E.; Fitt, W.K.; Schmidt, G.W. The effects of elevated temperature on the photosynthetic efficiency of zooxanthellae in hospite from four different species of reef coral: A novel approach. *Plant Cell Environ.* **1996**, *19*, 291–299. [[CrossRef](#)]
52. Matsubara, S.; Chow, W.S. Populations of photoinactivated photosystem II reaction centers characterized by chlorophyll a fluorescence lifetime in vivo. *Proc. Natl. Acad. Sci. USA* **2004**, *101*, 18234–18239. [[CrossRef](#)] [[PubMed](#)]

53. Kajiwara, K.; Nagai, A.; Ueno, S. Examination of the effect of temperature, light intensity and zooxanthellae concentration on calcification and photosynthesis of scleractinian coral *Acropora pulchra*. *J. Sch. Mar. Sci. Technol. Tokai Univ.* **1995**, *40*, 95–103.
54. Rodolfo-Metalpa, R.; Huot, Y.; Ferrier-Pagès, C. Photosynthetic response of the Mediterranean zooxanthellate coral *Cladocora caespitosa* to the natural range of light and temperature. *J. Exp. Biol.* **2008**, *211*, 1579–1586. [[CrossRef](#)] [[PubMed](#)]
55. Edmunds, P.J.; Brown, D.; Moriarty, V. Interactive effects of ocean acidification and temperature on two scleractinian corals from Moorea, French Polynesia. *Glob. Chang. Biol.* **2012**, *18*, 2173–2183. [[CrossRef](#)]
56. Warner, M.E.; Chilcoat, G.C.; McFarland, F.K.; Fitt, W.K. Seasonal fluctuations in the photosynthetic capacity of photosystem II in symbiotic dinoflagellates in the Caribbean reef-building coral *Montastraea*. *Mar. Biol.* **2002**, *141*, 31–38.
57. Anthony, K.R.N.; Hoegh-Guldberg, O. Kinetics of photoacclimation in corals. *Oecologia* **2003**, *134*, 23–31. [[CrossRef](#)] [[PubMed](#)]
58. Scheufen, T.; Kramer, W.E.; Iglesias-Prieto, R.; Enríquez, S. Seasonal variation modulates coral sensibility to heat-stress and explains annual changes in coral productivity. *Sci. Rep.* **2017**, *7*, 4937. [[CrossRef](#)] [[PubMed](#)]
59. Heron, S.F.; Liu, G.; Eakin, C.M.; Skirving, W.J.; Muller-Karger, F.E.; Vega-Rodriguez, M.; De La Cour, J.L.; Burgess, T.F.R.; Strong, A.E.; Geiger, E.F.; et al. *Climatology Development for NOAA Coral Reef Watch's 5-km Product Suite*; NOAA Technical Report NESDIS 145; NOAA/NESDIS: College Park, MD, USA, 2015.
60. Liu, G.; Rauenzahn, J.L.; Heron, S.F.; Eakin, C.M.; Skirving, W.J.; Christensen, T.R.L.; Strong, A.E.; Li, J. *NOAA Coral Reef Watch 50 km Satellite Sea Surface Temperature-Based Decision Support System for Coral Bleaching Management*; NOAA Technical Report NESDIS 143; NOAA/NESDIS: College Park, MD, USA, 2013.
61. Cooper, T.F.; Uthicke, S.; Humphrey, C.; Fabricius, K.E. Gradients in water column nutrients, sediment parameters, irradiance and coral reef development in the Whitsunday Region, central Great Barrier Reef. *Estuar. Coast. Shelf Sci.* **2007**, *27*, 503–519. [[CrossRef](#)]
62. Ignatov, A.; Zhou, X.; Petrenko, B.; Liang, X.; Kihai, Y.; Dash, P.; Stroup, J.; Sapper, J.; DiGiacomo, P. AVHRR GAC SST Reanalysis Version 1 (RAN1). *Remote Sens* **2016**, *8*, 315. [[CrossRef](#)]
63. Merchant, C.J.; Embury, O.; Roberts-Jones, J.; Fiedler, E.; Bulgin, C.E.; Corlett, G.K.; Good, S.; McLaren, A.; Rayner, N.; Morak-Bozzo, S.; et al. Sea surface temperature datasets for climate applications from Phase 1 of the European Space Agency Climate Change Initiative (SST CCI). *Geosci. Data J.* **2014**, *1*, 179–191. [[CrossRef](#)]



© 2017 by the authors. Licensee MDPI, Basel, Switzerland. This article is an open access article distributed under the terms and conditions of the Creative Commons Attribution (CC BY) license (<http://creativecommons.org/licenses/by/4.0/>).